>3PoA06-01<

Metal-as-Insulation REBCO Insert: Simplified Protection Scheme and Investigation of Cooling Defect under High-Field Operation

Jung-Bin Song, Xavier Chaud, François Debray, Steffen Krämer, Simon Bagnis,
Philippe Fazilleau, and Thibault Lécrevisse

***Abstract*—A refurbished metal-as-insulation (MI) HTS insert comprised of DP coils with replaced inner joints was charged under various magnetic field (B_{ext}) from 0 to 18 T at 4.2 K for testing. However, the refurbished insert could not be charged up to its maximum field, because the cryogenic condition tended to be unstable with a high helium boiling rate above 28 T. Therefore, to investigate the cooling issue, four Cernox sensors were installed in refurbished insert. The temperature of each position while powering the insert was measured under various B_{ext}. In addition, we qualified a new simplified protection scheme without the usual detection and dump circuit during a quench at B_{ext} = 9 T of the insert. Detailed experimental results about charging and quenching tests of the insert are presented and discussed in this paper.**

***Index Terms*—Helium bubble, HTS insert, Metal-as-insulation, Quench protection, REBCO coated conductor, Very-high-field.**

I. INTRODUCTION

To avoid local damage of the HTS magnet, removing the insulation between turns, the so-called no-insulation (NI) technique, has been proposed for allowing the current to bypass a local defective/quenched part in an HTS winding [1]. This self-protection feature considerably simplifies the protection scheme [1]-[7]. One major drawback is the resulting charging time as it takes an unreasonable time for the current to settle [8]-[15]. We improved this concept by introducing a residual resistance between turns by co-winding a stainless-steel (SS) tape with the HTS tape, the so-called metal-as-insulation (MI) technology [16]. The charging and discharging times are much improved as well as the mechanical robustness of the resulting metallic insulated HTS coil [17]-[19]. Based on this MI technique, we have constructed an MI HTS insert for development of a very-high-field magnet. In 2019, a hybrid magnet comprised of an HTS insert and a resistive outsert successfully reached 32.5 T, resulting from the combination of 14.5 T produced by the HTS and 18 T of resistive background field [20], [21]. After this achievement, the HTS insert was refurbished, because the insert experienced two major events provoking its quench, a fault of the resistive outsert at 28 T and a thermal runaway of the HTS insert at 32.5 T [22]. Thanks to our protection scheme comprised of MI winding and a dump resistor, the windings of the inserts survived these two quenches, but the HTS joining pieces used for the inner and outer electrical junctions underwent delamination and kinks. The refurbished insert was tested under various background fields (B_{ext}) at 4.2 K. However, it did not reach its maximum field, because the cryogenic condition tended to be unstable with a high helium boiling rate when above a total magnetic field (B_{ext}) of 28 T.

Since the previous tests, a 34 mm bore size SS tube was installed in the inner bore of the HTS insert for accessing the magnet center for NMR characterization or end-user sample mounting. Despite several openings, the circulation of liquid helium (LHe) inside the insert may be more difficult [22]. But more probably, a loss of cooling power has been linked to helium gas bubbles being trapped when the BdB_z/dz product reaches beyond 21 T²/cm [23]-[25].

Presently, we are conducting several projects to develop very-high-field LTS/HTS hybrid magnets in which this level is overpassed and therefore make the cooling problem highly pregnant. Therefore, in this study, four Cernox sensors were installed in the refurbished HTS insert to investigate the cooling issue. The temperature of each position around the charged HTS insert was measured under various B_{ext}. In addition, we took the opportunity of these new tests to qualify a new simplified protection scheme without the usual detection and dump circuit during a quench at B_{ext} = 9 T of the MI HTS insert. This new protection scheme avoids faulty triggering due to voltage spikes produced by conductor motion unavoidable in a dry winding coil and brutal transient associated with the opening of a power switch.

II. EXPERIMENTAL SET-UP

A. The refurbished HTS MI insert

The refurbished insert was comprised of 9 MI double

Submitted for review September 26, 2023

The authors acknowledge the support of the LNCMI-CNRS, member of the European Magnetic Field Laboratory (EMFL) and funding from the French ANR (Labex LANEF ANR-10-LABX-51-01 and PIA3 FASUM ANR-21-ESRE-0027) as well as from the European Union's Horizon 2020 research and innovation programme under grant agreement No 951714 (SuperEMFL project). *(Corresponding author: Xavier Chaud).*

J. B. Song, X. Chaud, F. Debray, and S. Krämer are with LNCMI-EMFL-CNRS, Univ. Grenoble Alpes, INSA, UPS, 38042 Grenoble, France (e-mail: jung-bin.song@lncmi.cnrs.fr; xavier.chaud@lncmi.cnrs.fr; francois.debray@lncmi.cnrs.fr; steffen.kramer@lncmi.cnrs.fr).

S. Bagnis, P. Fazilleau and T. Lécrevisse are with DACM, IRFU, CEA, Université Paris-Saclay, Gif sur Yvette, France (e-mail: simon.bagnis@cea.fr; philippe.fazilleau@cea.fr; thibault.lecrevisse@cea.fr).

Color versions of one or more of the figures in this article are available online at http://ieeexplore.ieee.org

pancake (DP) coils. The inner and outer diameter of the DP coils wound with REBCO tapes (75 µm thick and 6 mm wide) provided by SuperPower were 50 and 110.8 mm, respectively. The inductance and coil constant of the insert were 0.82 H and 44.3 mT/A, respectively. The refurbishing process and specification of the MI insert has already been described in detail in a previous paper [22]. Fig. 1 shows the experimental set-up for the tests. As seen in Fig. 1a, to investigate the position of trapped helium bubbles, four Cernox sensors were installed in the following locations: 1) one at the top of the stack of HTS pancake coils; 2) one at the bottom; 3) one at the external surface; and 4) one inside the inner bore closed to the top edge. Each sensor was covered with sticky paste (Patafix aka Blu-Tack) to hold it strongly in cryogenic temperature. Thermal contact is ensured by a little drop of Apiezon N grease. Several openings were machined into the 34 mm bore SS tube of the probe to allow helium penetration for improvement of thermal stability within the insert inner bore. The insert connected to its probe was installed in a cryostat with a 128 mm cold bore for immersion into a LHe bath at 4.2 K.

B. The resistive outsert installed in LNCMI-Grenoble

The MI HTS insert mounted into its cryostat was placed in the room temperature (RT) bore of a resistive magnet used as an outsert. Fig. 2 shows the outsert installed in the M10 room at LNCMI-Grenoble. The outsert with a 170 mm RT bore used for these tests consists of 2 Bitter stacks and 6 polyhelix coils. The maximum central field of the resistive outsert is 20 T (10 T Bitter and 10 T polyhelices) at a total power of 18 MW.

C. Concept of new protection scheme for the HTS insert

Fig. 3 shows two protection schemes for the MI HTS insert. In previous experiments, when the voltage of the insert

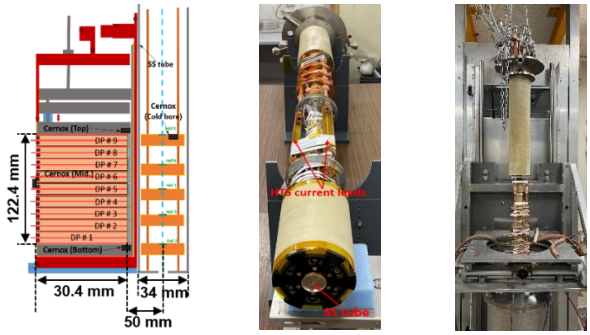

(a) (b) (c)

Fig. 1. Experimental set-up: the HTS insert (a); the insert connected to its probe (b); and the probe placed in the cryostat (c).

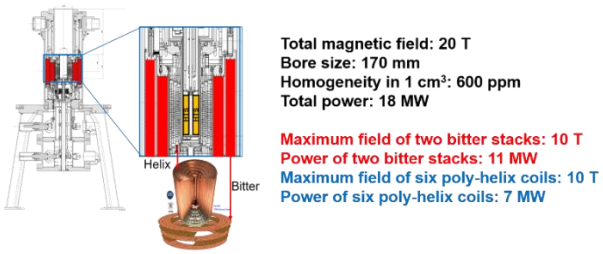

Fig. 2. 20 T/170 mm RT bore resistive outsert in LNCMI-G.

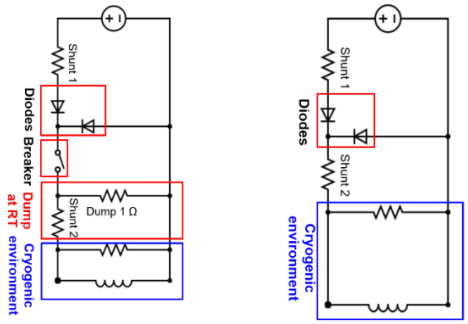

(a) (b)

Fig. 3. Protection schemes of the HTS insert: detect and dump technique (a); and PS voltage limitation technique (b).

exceeded a set threshold voltage, a mechanical switch was automatically opened, and the quench energy was dissipated into a dump resistor connected in parallel with the insert. In that case, because of the MI winding feature, when the current was bypassing a defect, the voltage to detect was about threefold higher than for an insulated winding, on the order of the mV rather than µV, therefore making the quench detection of MI windings significantly easier than that of insulated windings. In addition, when using thresholding protection, we could rely on a double security: 1) a Labview program that is monitoring the voltage difference between coils or a group of coils to correct for the inductive part of the signals; 2) the overvoltage function (shut-down) of the power supply (PS) when the voltage seen by the PS reached a set value.

However, this protection technique had two drawbacks. Firstly, the switch was often opened due to the voltage spikes caused by some unavoidable mechanical motions of the HTS dry windings under high magnetic field, resulting in unexpected sudden-discharge of high energy in the HTS insert. Secondly, when the switch was opened, the insert induced a very high transient that could generate large voltage spikes ($\geq$ 200 V) and/or mechanical shocks. In particular, the second drawback might be a critical issue for an LTS outsert which has a much larger inductance than the resistive outsert. Therefore, in this series of tests, to avoid unexpected sudden discharging and reduce voltage spikes of the HTS insert, we tried a new protection scheme based on the MI winding feature and the PS voltage limitation function (see figure 2b). As the voltage increase inside a MI insert is much faster and larger than in a conventional insulated HTS insert because of the current bypassing defects through high resistivity turns, the current delivered by the power supply will collapse to a value compatible with its set maximum voltage value. The set maximum voltage value on the PS does not even need to be accurately determined. The peak temperature due to quench reached similar value in simulation for 1 mV, 1 V or 5 V [26]. In this way, we can significantly and passively reduce the circulating current inside the insert from quench initiation, within the first few tens or hundreds of milliseconds. During this time, the metallic insulation tape serves the role of dump resistor for energy dissipation. Finally, we can safely turn off the PS while there are still only a few amperes circulating inside the insert.

III. Results and Discussion

A. *Investigating location of trapped helium bubble*

Fig. 4 shows charging test results of the MI insert at a current ramping rate of 0.5 A/s under B_{ext} = 10 T (a) and 18 T (b) at 4.2 K. It should be noted that 1) the result of B_{ext} = 18 T (Fig. 4b) was acquired from the previous tests [22]; and (2) the wires of the Cernox sensor attached on the external surface of the insert close to the midplane was broken probably due to motions of windings under very-high-field. In the case of B_{ext} = 10 T (Fig. 4a), the Joule heating at the resistive junction areas increased with increasing power supply current, but the temperatures remained stable up to the B_{tot} of 19 T. From 20 T, the temperature of the insert's top area connected with the negative current lead (NCL) began to increase, while the temperature of the insert's bottom connected with the positive current lead (PCL) remained stable. This probably indicates helium bubbles trapped close to the top area, resulting in inefficient cooling for the insert. Note: Voltage of connection between PCL and bottom DP coil is much higher than that of connection between NCL and top DP coil, which implies that the voltages had no correlation with temperature increase of the insert. When the total magnetic field exceeded 22 T (insert current of 290 A), the top temperature of the insert rapidly increased. And the bottom temperature of the insert also started to rise because the trapped helium bubbles accumulated in the top area into an increasing gas pocket and disturbed the LHe circulation towards the bottom. When the field was then reduced, the temperature keeps increasing because field ramping is always a source dissipation due to induced currents in the winding and transient radial currents.

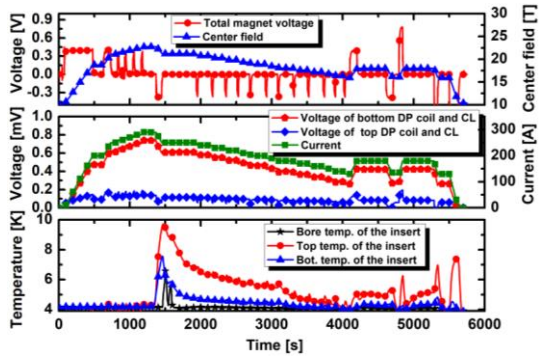

(a)

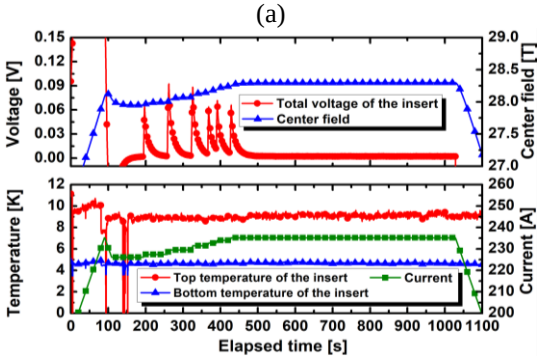

(b)

Fig. 4. Charging/discharging test results of the MI HTS insert under: B_{ext} = 10 T (a); and 18 T (b) in bath of LHe at 4.2 K.

However, once the plateau at a lower field was reached, the temperature started to decrease. In addition, at 1460 seconds, the bottom and top temperatures of the insert decreased, while the temperature in the magnet's cold bore increased. This is probably ascribed to the migration of released helium bubbles. As the magnetic field decreased further, the magnetic gradient decreased, resulting in a reduction in the trapped bubble regions. Thermal exchange was resumed, and a new equilibrium between cooling and local Joule heating effects was established at lower temperatures. In the graph part after 4200 seconds, it was observed that the temperature becomes unstable when increasing the currents back to 180 A. In the case of B_{ext} = 18 T (Fig. 4b), the magnetic field produced by the insert was 10.2 T at 235 A, yielding a combined field of 28.2 T. Compared to the maximum field in Fig. 4a, despite the higher maximum field of 6 T, the bottom temperature of the insert remained very stable (4.2 K). The reasons are as follows: Firstly, during this test, the helium bath was pumped, making it easier for the LHe circulation towards the bottom. Secondly, the maximum charging current of the insert was approximately 51 A lower than the maximum current in Fig. 4a, resulting in lower Joule heating at junction area between positive current lead and bottom winding. Meanwhile, the top temperature of the insert remained at 9 K despite pumping, indicating that helium bubbles were trapped in the vicinity of the top region, and operation of the pumping system did not effectively eliminate the helium bubbles.

To confirm location of trapped helium bubble, we performed simulation. The region of trapped helium bubbles can be calculated by $B_z \cdot dB_z/dz$ < -2100 T^2/m [23]-[25], where B_z and Z are the axial magnetic field and the axial direction of the magnet, respectively. Here, we considered the shape of fluid pressure well for compensation [27]. Fig. 5 shows simulation results of trapped bubbles position under the same maximum fields of the insert and outsert as in Fig. 4. As seen in Fig 5a, starting from the center of the insert inner bore, trapped helium bubble region (white color) is formed up to its top area, while the bottom region remains covered with LHe (blue color). In addition, a temperature sensor located at the inner bore of the insert was placed within the trapped helium area; however, the temperature was very stable during the test (see black star of Fig. 4a). The reason is that, unlike the top and bottom areas of the HTS insert where Joule heating occurred due to resistance junctions, the inner bore area did

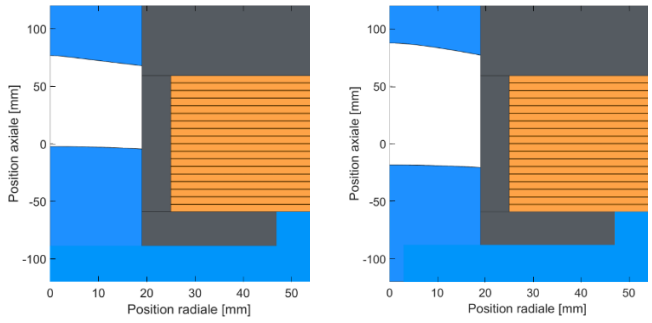

(a) (b)

Fig. 5. Simulation results of trapped bubble position under same condition in Fig. 4: B_{ext} = 10 T (a); and 18 T (b) at 4.2 K.

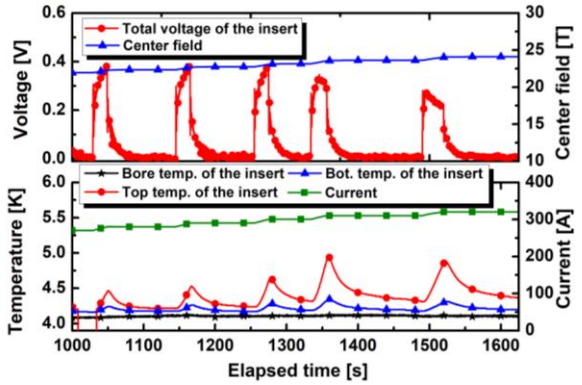

Fig. 6. Charging test result of the MI insert under 10 T external field generated by only bitter stacks at 4.2 K.

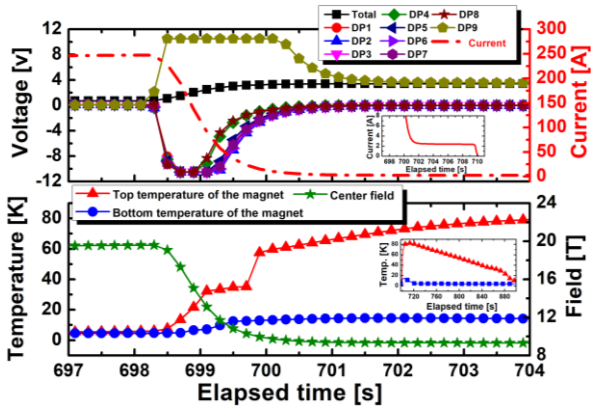

Fig. 7. Quench protection behavior of the insert with MI winding and PS voltage limitation techniques at I_{op} = 247 A under B_{ext} = 9 T at 4.2 K.

not have any source of heating, so the temperature was very stable even in the trapped helium bubble area. As seen in Fig 5 (b), the trapped helium bubble region expanded in both the upward and downward directions as the magnetic field increased. However, the bottom region of the insert is still covered by LHe.

To investigate the thermal stability of the HTS insert during the operation of the resistive outsert in only Bitter stacks operation, we turned off the power of the polyhelix coils. Fig. 6 shows a charging test result of the MI insert under only a Bitter external field (B_{bit}) of 10 T at 4.2 K. The insert was charged up to 14 T at 318 A, giving a B_{tot} of 24 T. The maximum temperatures of top and bottom areas were 4.9 and 4.3 K, respectively. Moreover, at a plateau of 24 T, the temperature of the top area was decreasing towards 4.2 K, which indicates the insert is more thermally stable in an external magnetic field produced by only the Bitter stacks. This is because the field gradient of the Bitter stacks alone is smoother than the one obtained by the polyhelices-Bitter co-operation, so the region of trapped helium bubble is relatively smaller.

As it seems difficult to reduce *dB*/*dz* sufficiently to balance the increasing value of B, a better understanding of the helium circulation is mandatory for future development of very-high-field magnet. Conduction cooling may be a solution at the sake of temperature margin.

B. Quench protection behavior using PS voltage limitation

Fig. 7 demonstrates the quench protection behavior of the insert with MI winding and PS voltage limitation techniques at I_{op} = 247 A under B_{ext} = 9 T at 4.2 K. To limit the PS current during quench, we set the PS voltage limitation at 3.5 V, which is slightly above the maximum voltage expected from the resistance of the whole system including current leads and MI insert. As seen in Fig. 7, as the DP 9 voltage increased, the voltages of the other DP decreased to maintain the total induction. The current (red dash-dot curve) and the magnetic field (green star) decreased as soon as the voltage increased (black square). This is because as the insert voltage increased, the PS voltage also increased, resulting in an automatic collapse of the PS current. The current was finally limited to about 3 A at total magnet voltage of 3.5 V during 10 s before the PS was switched off. In addition, the quench energy was also automatically dissipated (measured maximum temperature of the insert: 82 K) within the MI windings through turn-to-turns contacts. After this event, the damage of the insert was evaluated by comparing new charging tests with previous one: no abnormal signals from the insert were observed. This result demonstrates that the proposed technique comprised of MI winding and PS voltage limitation can protect HTS insert against quench without high voltage peak and unintended sudden discharge event.

IV. Conclusion

In this paper, trapped helium bubble location of a 38 mm cold bore metal-as-insulation (MI) HTS insert was investigated via experimental and simulation works. In addition, a new simplified protection scheme comprised of MI winding and a power supply (PS) voltage limitation technique was tested to estimate its feasibility. Based on the test results, the conclusions can be summarized as follows:

- The experimental results agreed well with simulation results. The thermal stability of the insert at its top area was much lower than at its bottom area, because the helium gas bubbles were mainly trapped upward from the center of the insert inner bore close to the top edge of the insert. In addition, when pumping, the temperature of the bottom part of the insert becomes very stable, but the top temperature of the insert was still high (about 9 K), which means that pumping is not effective for eliminating the trapped zone. Therefore, the related cooling issue has to be seriously considered for the development of very high field magnets.
- During a quench of the insert, the current of the PS can be automatically collapsed by the combination of the PS voltage limit with the high voltage increase of MI windings due to radial currents bypassing a defective or quenched part of the coil. The quench energy was dissipated (measured maximum temperature of the insert: 82 K) only within the windings without any damage of the insert. This result demonstrates that the proposed technique which is rather simple to implement can effectively protect an insert against quench without high voltage peak while avoiding triggering unexpected sudden discharge.

REFERENCES

[1] S. Hahn, D. K. Park, J. Bascuñán, and Y. Iwasa, "HTS pancake coils without turn-to-turn insulation," *IEEE Trans. Appl. Supercond*., vol. 21, no. 3, pp. 1592–1595, Jun. 2011.

[2] Y. Yanagisawa, K. Sato, K. Yanagisawa, H. Nakagome, X. Jin, M. Takahashi, and H. Maeda, "Basic mechanism of self-healing from thermal runaway for uninsulated REBCO pancake coils," *Physica C*, vol. 499, pp. 40-44, Apr. 2014.

[3] D. H. Kang, K. L. Kim, Y. G. Kim, Y. J. Kim, Y. J. Park, W. J. Kim, S. H. Kim, and H. G. Lee, "Investigation of thermal and electrical stabilities of a GdBCO coil using grease as an insulation material for practical superconducting applications," *Rev. Sci. Instrum.* vol. 85, no. 9, p. 094701, Sep. 2014.

[4] T. Wang, S. Noguchi, X. Wang, I. Arakawa, K. Minami, K. Monma, A. Ishiyama, S. Hahn, and Y. Iwasa, "Analyses of transient behaviors of no-insulation REBCO pancake coils during sudden discharging and overcurrent," *IEEE. Trans. Appl. Supercond*., vol.25, no. 3, p. 4603409, Jun. 2015.

[5] S. Choi, H. C. Jo, Y. J. Hwang, S. Hahn, and T. K. Ko, "A study on the no insulation winding method of the HTS coil," *IEEE Trans. Appl. Supercond.*, vol. 22, No. 3, p. 4904004, Jun. 2012.

[6] X. Wang, S. Hahn, Y. Kim, J. Bascuñán, J. Voccio, H. G. Lee, and Y. Iwasa, "Turn-to-turn contact characteristics for an equivalent circuit model of no-insulation ReBCO pancake coil," *Supercond. Sci. Technol.*, vol. 26, No. 3, p. 035012, Mar. 2013.

[7] J. B. Song, S. Hahn, Y. Kim, D. Miyagi, J. Voccio, J. Ling, J. Bascuñán, H. G. Lee, and Y. Iwasa, "Dynamic responses of no-insulation and partial-insulation coils for HTS wind power generator," *IEEE. Trans. Appl. Supercond*., vol.25, no. 3, p. 5202905, Jun. 2015.

[8] J. B. Song, S. Hahn, T. Lécrevisse, J. Voccio, J. Bascuñán, and Y. Iwasa, "Over-current quench test and self-protecting behavior of a 7 T/78 mm multi-width no-insulation REBCO magnet at 4.2 K," *Supercond. Sci. Technol.* vol. 28, p. 114001, Sep. 2015.

[9] Y. H. Choi, K. L. Kim, O. J. Kwon, D. H. Kang, J. S. Kang, T. K. Ko, and H. G. Lee, "The effects of partial insulation winding on the charge–discharge rate and magnetic field loss phenomena of GdBCO coated conductor coils," *Supercond. Sci. Technol.*, vol. 25, No. 10, p. 105001, Jul. 2012.

[10] J. B. Song, S. Hahn, Y. Kim, J. Voccio, J. Ling, J. Bascuñán, H. G. Lee, and Y. Iwasa, "HTS Wind Power Generator: Electromagnetic force between no-insulation and insulation coils under time-varying conditions," *IEEE. Trans. Appl. Supercond*., vol.24, no. 3, p. 5201005, Jun. 2014.

[11] Y. Wang, H. Song, D. Xu, Z. Y. Li, Z. Jin, and Z. Hong, "An equivalent circuit grid model for no-insulation HTS pancake coil," *Supercond. Sci. Technol.*, Vol. 28 p. 045017, Mar. 2015.

[12] J. Y. Jang, S. Yoon, S. Hahn, Y. J. Hwang, J. Kim, K. H. Shin, K. Cheon, K. Kim, S. In, Y. Hong, H. Yeom, H. Lee, S. Moon, and S. Lee, "Design, construction and 13 K conduction-cooled operation of a 3 T 100 mm stainless steel cladding all-REBCO magnet," *Supercond. Sci. Technol.* vol. 30, p. 105012, Sep. 2017.

[13] S. Kim, S. Hahn, K. Kim and D. Larbalestier, "Method for generating linear current-field characteristics and eliminating charging delay in no-insulation superconducting magnets," *Supercond. Sci. Technol*. vol. 30, p. 035020, Feb. 2017.

[14] J. B. Song and S. Hahn, "Leak current correction for critical current measurement of no-insulation HTS coil," Progress in Superconductivity and Cryogenics, vol.19. no2, pp. 48~52, 2017.

[15] D. Liu, H. Yong, and Y. Zhou, "Analysis of charging and sudden discharging characteristics of no-insulation REBCO coil using an electromagnetic coupling model," *AIP Advance*, vol. 7, p. 115104, Nov. 2017.

[16] T. Lécrevisse and Y. Iwasa, "A(RE)BCO pancake winding with metal-as-insulation," *IEEE. Trans. Appl. Supercond*., vol.26, no. 3, p. 4700405, Jun. 2016.

[17] T. Lécrevisse, A. Badel, T. Benkel, X. Chaud, P. Fazilleau, and P. Tixado, "Metal-as-insulation variant of no-insulation HTS winding technique: pancake tests under high background magnetic field and high current at 4.2 K," *Supercond. Sci. Technol*. vol. 31, no. 5, p. 055008, Apr. 2018

[18] P. Fazilleau, B. Borgnic, X. Chaud, F. Debray, T. Lécrevisse, and J. B. Song, "Metal-as-insulation sub-scale prototype tests under a high background magnetic field," *Supercond. Sci. Technol*. vol. 31, no. 9, p. 095003, Jul. 2018.

[19] J. B. Song, X. Chaud, B. Borgnic, F. Debray, P. Fazilleau, and T. Lécrevisse, "Construction and test of a 7 T metal-as-insulation HTS insert under a 20 T high background magnetic field at 4.2 K," *IEEE Trans. Appl. Supercond.*, vol. 29, No. 5, p. 4601705 (5pp), Aug. 2019.

[20] P. Fazilleau, X. Chaud, F. Debray, T. Lécrevisse, and J. B. Song, "38 mm diameter cold bore metal-as-insulation HTS insert reached 32.5 T in a background magnetic field generated by resistive magnet," *Cryogenics*, vol. 106, p. 103053, Feb. 2020.

[21] T. Lécrevisse, X. Chaud, P. Fazilleau, C. Genot, and J. B. Song, "Metal-as-insulation HTS coil," *Supercond. Sci. Technol.*, vol. 35, no. 7, p074004, May 2022.

[22] J. B. Song, X. Chaud, F. Debray, S. Krämer, P. Fazilleau, and T. Lécrevisse, "Metal-as-insulation HTS insert for very-high-field magnet: a test report after repair ," *IEEE Trans. Appl. Supercond.*, vol. 32, No. 6, p. 4300206, Sep. 2022.

[23] McNiff et al., "Temperature anomalies observed in liquid 4He columns in magnetic fields with field-field-gradient products > 21 T²/cm", *Rev. Sci. Instrum.* **59** (1988) 2474

[24] H. Bai, S. T. Hannahs, W. D. Markiewicz, and H. W. Weijers, "Helium gas bubble trapped in liquid helium in high magnetic field," *Appl. Phys. Lett.*, vol. 104, p. 133511, Nov. 2014.

[25] H. Bai, W. D. Markiewicz, H. W. Weijers, A. Voran, P. D. Noyes, B. Jarvis, W. R. Sheppard, Z. L. Johnson, S. R. Gundlach, and S. T. Hannahs, "Impact of trapped helium gas bubble in liquid helium on the cooling in high magnetic field," *IEEE Trans. Appl. Supercond.*, vol. 25, No. 3, p. 4300104, June 2015.

[26] C. Genot, "Numerical and experimental studies for the optimization and protection of NI-MI HTS coils," Ph.D. dissertation, the electronics, electrotechnics, automation, signal processing doctoral school, University of Grenoble-Alpes, Grenoble, France, 2022.

[27] S. Bagnis, "Study of the influence of magneto-gravitational forces on liquid helium cooling of superconducting magnets with high magnetic fields," Ph.D. dissertation, Dept. Elect. Eng. University of Paris-Saclay, Gif sur Yvette, France, 2023.